

Characterization of Multi-Carrier Heterostructure Devices with Quantitative Mobility Spectrum Analysis and Variable Field Hall Measurements

J. R. Lindemuth, Gang Du, and B. C. Dodrill

Lake Shore Cryotronics, Inc., 575 McCorkle Boulevard, Westerville, OH 43082, USA

K. Vargason and Y. C. Kao

Intelligent Epitaxy Technology, Inc., 201 East Arapaho Rd., Ste 200, Richardson, TX 75081, USA

I. Vurgaftman, and J. R. Meyer

Code 5613, Naval Research Lab, Washington, DC 20375, USA

Abstract. Hall measurements at a single applied magnetic field are incapable of characterizing the multi-carrier properties of heterostructure devices such as HEMT and multi-quantum wells because the measured parameters are averaged over all carriers. In this paper, we demonstrate a novel characterization technique, Quantitative Mobility Spectrum Analysis (QMSA) in conjunction with variable magnetic field Hall measurements that provides for the extraction of individual carrier mobilities and densities for multi-carrier devices. Temperature (2 - 400 K) and magnetic field (0 - 9 T) dependent Hall measurements and QMSA results for InP HEMT devices will be presented. For the HEMT device, the high mobility 2DEG carrier in the quantum well channel layer and the doped cap layer carrier are clearly distinguished and their properties are extracted by QMSA. Temperature-dependent properties of the individual carriers may also be determined using this technique, and such measurements provide insight into the multi-quantum well device properties at low temperatures. The reliability and sensitivity of QMSA and variable field measurements show that this technique is a powerful measurement methodology for routine electrical characterization of multi-carrier semiconductor devices for both research and industrial QC/QA applications.

Introduction

Advances in compound semiconductors have resulted in novel heterostructure devices with superior performance. These devices are widely used in RF, microwave, and optical applications today. The rapid pace with which these device technologies have advanced have, in turn, necessitated the development of new measurement and data analysis techniques. For example, conventional single magnetic field Hall characterization is incapable of providing a precise determination of the electronic transport properties of a multi-layered device such as a pHEMT. The key parameters of a pHEMT are mobility and density of the 2DEG carrier (or carriers) in the quantum well channel layer. In order to characterize the 2DEG carrier in a pHEMT device with single field Hall measurement techniques, one has to either repeat the steps of etching and characterizing until the doped cap layer is removed, or terminate the epi growth process before the cap layer is formed.

Even if these steps are taken, the accuracy of the characterization cannot be guaranteed if additional carrier(s) such as surface and interface charges exist in the measured sample.

In this paper, we demonstrate a novel multi-carrier characterization technique, the quantitative mobility spectrum analysis (QMSA),¹⁻⁶ which is an improvement over previous spectrum data analysis approaches.^{7,8} Similar to two other mixed conduction analysis techniques, finite number carrier least-square fit⁹ and Shubnikov-de Haas (SdH) effect,¹⁰ this technique analyzes variable magnetic field Hall data. QMSA complements these two methods, but also provides significant advantages. For example, the finite number carrier fit method requires knowledge of the number of carriers in advance, whereas fully automated QMSA requires no advance sample information and is capable of providing mobilities and densities with accuracy comparable to the finite number fit technique. Although the SdH technique can in some cases extract individual carrier densities in

a multi-carrier sample that displays multiple oscillation periods, unlike QMSA it cannot provide mobility values.

In this work, we apply QMSA to synthetic multi-carrier Hall data, and also to variable field Hall measurement data for an InP pHEMT device from Intelligent Epitaxy Technology. The results show that this technique extracts individual carrier mobilities and densities for multi-carrier materials, and is especially reliable and sensitive for high mobility heterostructure devices such as pHEMTs. Data for devices with cap layers will be compared to devices without cap layers. This will demonstrate QMSA's ability to resolve multi-carriers in pHEMTs. Comparison with the results of SdH measurements will be discussed.

QMSA

1. Theoretical background

For a single carrier material, the measured Hall coefficient and resistivity are given by,¹¹

$$R_H(B) = \frac{1}{nq} \quad (1)$$

$$\rho(B) = \frac{1}{nq\mu}, \quad (2)$$

and the conductivity tensor is given by,

$$\sigma_{xx} = \frac{nq\mu}{1 + \mu^2 B^2} \quad (3)$$

$$\sigma_{xy} = \frac{nq\mu^2 B}{1 + \mu^2 B^2}. \quad (4)$$

Here n is the carrier concentration, μ is the mobility, q is the charge of the carrier, and B is the magnetic field. It is apparent from Eqs. (1) and (2) that for single carrier materials the Hall coefficient and resistivity are field independent. The single field Hall characterization is therefore sufficient for such materials.

However, for multi-carrier systems the mobility and density calculated from Eqs. (1) and (2) will be averaged over all carriers. For such materials, conductivities of the individual carriers are additive, and the total conductivity tensor (of a N -carrier system) is given by:²

$$\sigma_{xx} = \sum_i^N \frac{n_i q_i \mu_i}{1 + \mu_i^2 B^2} \quad (5)$$

$$\sigma_{xy} = \sum_i^N \frac{n_i q_i \mu_i^2 B}{1 + \mu_i^2 B^2} \quad (6)$$

The finite number carrier analysis performs a least-square fit of the measured data to a preset number of carriers. In this approach, the number

of carriers N must be defined in advance and (μ_i, n_i) of each carrier are fitting parameters.

This shortcoming can be overcome by using the "mobility spectrum" concept. In this approach, discrete carriers are generalized by a conductivity density function that spreads over a continuous mobility range. The conductivity tensor is given by:¹²

$$\sigma_{xx} = \int_{-\infty}^{\infty} \frac{s^p(\mu) + s^n(\mu)}{1 + \mu^2 B^2} d\mu \quad (7)$$

$$\sigma_{xy} = \int_{-\infty}^{\infty} \frac{(s^p(\mu) - s^n(\mu))\mu B}{1 + \mu^2 B^2} d\mu \quad (8)$$

where $s^p(\mu)$, $s^n(\mu)$ are hole and electron conductivity density functions, respectively. The QMSA analysis technique improves greatly over earlier efforts utilizing the spectrum concept.^{7,8} For detailed discussions of QMSA and its applications, please refer to References 1-6.

2.A two-carrier test of QMSA

Figure 1 shows synthetic Hall data for a two-electron-carrier case over the magnetic field range 0.005 - 5 T. The mobilities and densities of the two electron carriers are listed in Fig. 1. A random uncertainty of 0.05% is added to the data. A single field measurement at 0.35 T (using the data from Fig. 1a) would have yielded a mobility of -3.98×10^3 cm²/Vs and density of -4.47×10^{13} cm⁻³, which clearly do not reflect either of the two carriers.

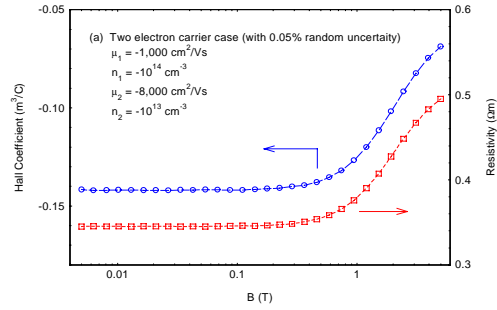


Figure 1. Synthetic Hall data of the two-carrier case.

Figure 2 plots the QMSA spectrum result for this example. Two well-separated electron peaks representing the two carriers are shown in the spectrum. The mobility and density values (listed in Figure 2) of these two peaks extracted by QMSA match the two set carriers to within 1%.

Figure 2 also shows a small hole peak. This is an analysis artifact due to the limited field range and measurement uncertainty. Increasing the range of magnetic fields over which measurements are conducted tends to minimize the occurrence of such artifacts. Furthermore, these artifacts are usually much smaller in

magnitude than the dominant peaks and their contribution to the total conductivity is negligible.

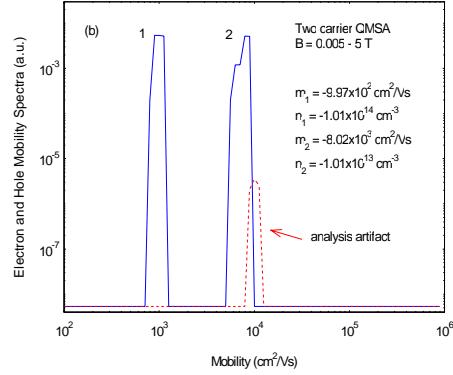


Figure 2. QMSA spectrum results for data in Figure 1. The solid curve represents electrons and dashed curve represents holes (same for all the QMSA plots below).

3. A four-carrier test of QMSA

Figure 3 plots the QMSA spectrum result for a synthetic four-carrier case (three electrons and one hole with a random uncertainty of 0.05%). The magnetic field range for this data set extends from 0.009 to 9 T. In addition to minimizing the artifacts discussed above, higher field strength is needed to improve the QMSA resolution when a large number of carriers are present, particularly when their mobilities are similar in value. For this model case, all four carriers are readily extracted by QMSA. The set mobilities and densities of the four carriers and the corresponding QMSA results are listed in Table I. The accuracy of the QMSA results in this case is slightly poorer than in the two-carrier case, but is still quite reasonable.

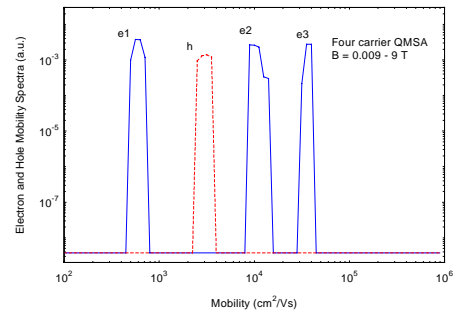


Figure 3. The four-carrier case QMSA spectrum.

	μ_{set} cm^2/Vs	μ_{QMSA} cm^2/Vs	n_{set} cm^{-3}	n_{QMSA} cm^{-3}
e1	-600	-601	-1e14	-1.00e14
e2	-1e4	-1.02e4	-5e12	-5.01e12
e3	-3.7e4	-3.75e4	-1e12	-9.66e11
h	3e3	3.03e3	1e13	1.00e13

Table I. The four-carrier case set mobilities and densities and their corresponding QMSA results.

Experiment

Variable field Hall and SdH measurements were conducted on InP PHEMT devices, fabricated by Intelligent Epitaxy Technology, using the Lake Shore Hall Measurement System (HMS) Model 9509. One device was fabricated with a cap layer; the other was fabricated without a cap layer. HMS 9509 is a superconducting cryogenic system with a maximum field of 9 T and temperature range of 2 - 400 K.

A van der Pauw sample configuration with four contacts was used to conduct the measurements. Gold wires were heat-bonded to gold contact pads, providing ohmic contacts as assured via two-probe I-V curve measurements, which were linear.

Measurement results

1. Variable field Hall measurements and QMSA results.

Variable field Hall measurements were conducted for fields from 200 G to 85 KG (0.02 to 8.5 T) and at various temperatures. Figures 4 and 5 show the measured sheet resistivity and the measured sheet Hall coefficient data at 50 K and 300 K. for a sample with a cap (figure 4) and a sample without a cap (figure 5). For the sample with out a cap, the field dependency of the data is small. From the observation we would conclude that one carrier is contributing to the conduction. However for the device with a cap (figure 4) the field dependency is quit large and we would expect more than one carrier to contribute to the conductivity. Figures 6 (sample with cap) and 7 (sample with out cap) shows the derived conductivity tensor and the fitted results from QMSA. The near perfect fit (solid lines) to the data is a good indication of the validity of the QMSA spectrum results presented below.

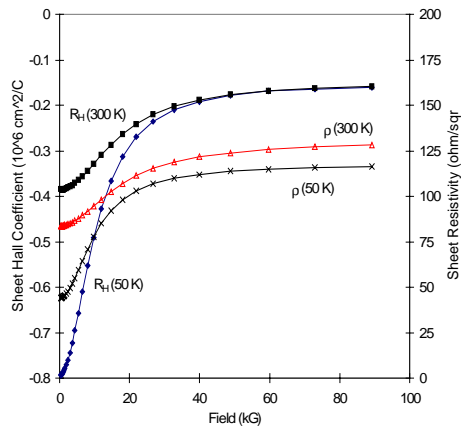


Figure 4. Measure sheet resistivity and sheet Hall coefficient of device with cap layer. The lines are guides for the eyes.

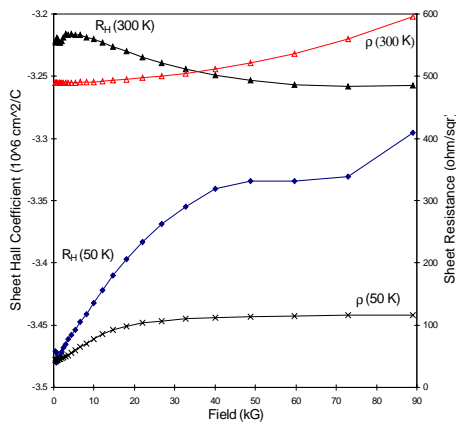


Figure 5. Measured sheet resistivity and sheet Hall coefficient of device with no cap layer. As expected this device shows less field dependency than the device in Figure 4.

Application of QMSA to the measured Hall data shown in the figures results in the multi-carrier mobility spectra plotted in Figure 8. As expected, the spectrum for the sample without a cap shows only one electron carrier. At a temperature of 50K the mobility is $21000 \text{ cm}^2/(\text{V s})$ and the sheet density is $1.75 \times 10^{12} \text{ cm}^{-2}$. However, at 300 K the mobility has decreased to 6600. The sheet density remains relatively constant at 1.89×10^{12} . This decrease in mobility with temperature is consistent with electron-phonon scattering.

In contrast, the sample with the cap shows the same carrier as the sample without the cap, but there is now a second electron carrier, in the cap layer, with low mobility. At 50K this carrier has a mobility of $1100 \text{ cm}^2/(\text{V s})$ and a

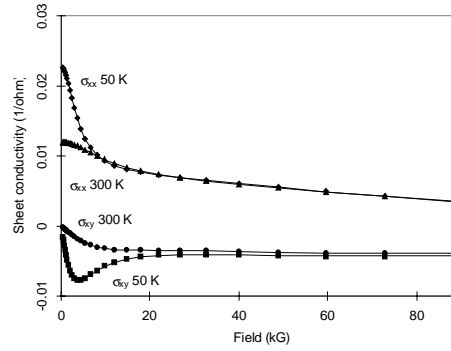


Figure 6. Conductivity calculated from the data in Figure 4. The symbols are the experimental data and the lines are the fits from QMSA.

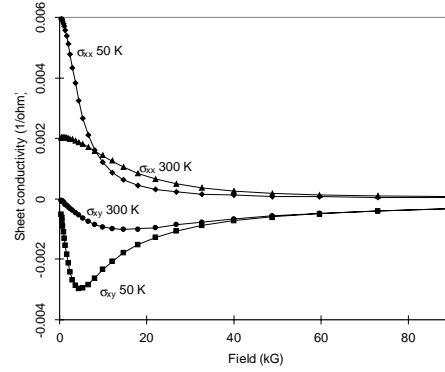


Figure 7. Conductivity calculated from the data shown in Figure 5. The symbols are the experimental data and the lines are fits from QMSA.

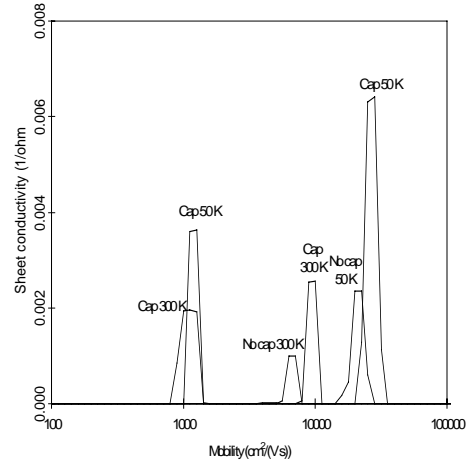


Figure 8. QMSA spectrum for both InP samples, with cap and without cap. The sample with out a cap shows one carrier with a temperature dependent mobility. The mobility changes from 21000 (at 50 K temperature) to 6600 (at 300 K temperature). The sample with a cap has only two carriers. One with mobility of about 10000 and a second with mobility of about 1000. The second carrier (the one in the cap) shows little temperature dependence

sheet density of $3.77 \times 10^{13} \text{ cm}^{-2}$. At 300 K its mobility is $1000 \text{ cm}^2/(\text{V s})$ and sheet density is $3.80 \times 10^{13} \text{ cm}^{-2}$. The high mobility carrier changes slightly with the application of the cap. At 300 K the mobility is $9400 \text{ cm}^2/(\text{V s})$ and the sheet density is $3.4 \times 10^{12} \text{ cm}^{-2}$. Although these are two different samples which could account for the difference, there is also a fundamental difference that is due to the changes in the electrostatic fields in the device because of the cap.

The mobility of the highest mobility peak increases with decreasing temperature, indicating that electron-phonon scattering dominates the charge transport in the channel layer. The temperature dependence of the mobility of the 2DEG carrier in the sample with the cap is shown in Figure 9.

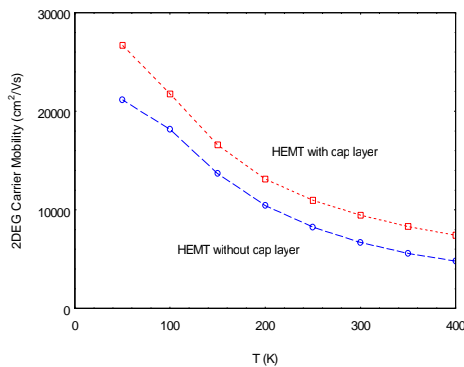


Figure 9. Temperature dependence of highest mobility carrier. This indicates that electron-phonon scattering dominates the transport process.

2. SdH effect measurement results

Figure 10 shows the SdH measurement result at 4.2 K. This measurement was done on the sample with out a cap. A Fourier transform analysis of these data reveals, as expected, one frequency, that yields a carrier density of $n_1 = 1.6 \times 10^{12} \text{ cm}^{-2}$. This carrier agrees with the densities corresponding to the two highest mobility features in the QMSA spectra of Figure 8.

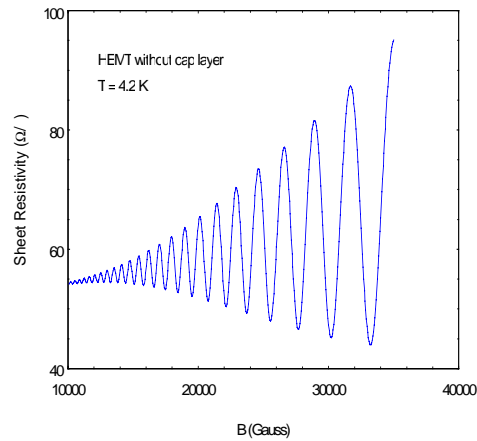


Figure 10. SdH measurement at 4.2 K. Single oscillation is consistent the one carrier model of the sample without cap. The corresponding sheet density is $1.6 \times 10^{12} \text{ cm}^{-2}$.

Conclusion

We have demonstrated that variable field Hall measurements and the fully automated QMSA are capable of providing much more information than single-field data when applied to multi-carrier devices. QMSA is especially powerful in characterizing high mobility devices such as pHEMTs and multi quantum wells. For the present InP pHEMT device, QMSA easily separates the high mobility 2DEG carrier(s) from the low mobility species. Measurements on two pHEMT samples, one with a cap and one with out, clearly demonstrate QMSA ability to accurately determine the number of carriers and the density and mobility of each carrier. The advantage of using variable field Hall measurements and QMSA in routine production QA/QC and device R&D for heterostructure materials, rather than conventional single-field Hall characterization methods, has been clearly demonstrated.

Acknowledgments

Discussion with Fred Pollak is gratefully acknowledged. Work at the Naval Researcher Lab was supported in part by a Cooperative Research and Development Agreement with Lake Shore Cryotronics, Inc.

References

1. J. Antoszewski, D. J. Seymour, L. Faraone, J. R. Meyer, and C. A. Hooman, *J. Electron. Mater.* 24, 1255 (1995).
2. J. R. Meyer, C. A. Hoffman, F. J. Bartoli, D. J. Arnold, S. Sivanathan, and J. P. Faurie, *Semicon. Sci. Technol* 8, 805 (1993).
3. J. R. Meyer, C. A. Hoffman, J. Antoszewski, and L. Faraone, *J. Appl. Phys.* 81, 709 (1997).
4. I. Vurgafman, J. R. Meyer, C. A. Hoffman, D. Redfern, J. Antoszewski, L. Faraone, and J. R. Lindemuth, *J. Appl. Phys.* 84, 4966 (1998).
5. B. J. Kelley, B. C. Dodrill, J.R. Lindemuth, G. Du, and J. R. Meyer, *Solid State Technol.* 12, 130 (2000).
6. B. C. Dodrill, J. R. Lindemuth, B. J. Kelley, G. Du, and J. R. Meyer, *Compound Semicond.* 7, 58 (2001).
7. W. A. Beck and J. R. Anderson, *J. Appl. Phys.* 62, 541 (1987).
8. Z. Dziuba and M. Gorska, *J. Phys. III France* 2, 99 (1992).
9. D. C. Look, C. E. Stutz, and C. A. Bozada, *J. Appl. Phys.* 74, 311 (1993).
10. L. M. Roth and P. N. Argyres, *Semiconductor and Semimetals*, vol. 1, ed. by R. K. Willardson and A. C. Beer (Academic, New York, 1966) p.159.
11. E. H. Putley, *The Hall Effect* (Butterworth, London, 1960).
12. W. A. Beck and J. R. Anderson, *J. Appl. Phys.* 62, 541 (1987).